Nuclear Instruments and Methods in Physics Research A 602 (2009) 618–621

Contents lists available at ScienceDirect

Nuclear Instruments and Methods in Physics Research A

journal homepage: www.elsevier.com/locate/nima

# A multi-threshold sampling method for TOF-PET signal processing

H. Kim [a,*], C.M. Kao [a], Q. Xie [a], C.T. Chen [a], L. Zhou [b], F. Tang [b], H. Frisch [b], W.W. Moses [c], W.S. Choong [c]

[a] Department of Radiology, University of Chicago, Chicago, IL 60637, USA
[b] Enrico Fermi Institute, University of Chicago, Chicago, IL 60637, USA
[c] Lawrence Berkeley National Laboratory, Berkeley, CA 94720, USA

ARTICLE INFO

*Article history:*
Received 6 January 2009
Accepted 19 January 2009
Available online 4 February 2009

*Keywords:*
Positron emission tomography
Multi-threshold sampling
Time resolution

ABSTRACT

As an approach to realizing all-digital data acquisition for positron emission tomography (PET), we have previously proposed and studied a multi-threshold sampling method to generate samples of a PET event waveform with respect to a few user-defined amplitudes. In this sampling scheme, one can extract both the energy and timing information for an event. In this paper, we report our prototype implementation of this sampling method and the performance results obtained with this prototype. The prototype consists of two multi-threshold discriminator boards and a time-to-digital converter (TDC) board. Each of the multi-threshold discriminator boards takes one input and provides up to eight threshold levels, which can be defined by users, for sampling the input signal. The TDC board employs the CERN HPTDC chip that determines the digitized times of the leading and falling edges of the discriminator output pulses. We connect our prototype electronics to the outputs of two Hamamatsu R9800 photomultiplier tubes (PMTs) that are individually coupled to a $6.25 \times 6.25 \times 25\,mm^3$ LSO crystal. By analyzing waveform samples generated by using four thresholds, we obtain a coincidence timing resolution of about 340 ps and an ~18% energy resolution at 511 keV. We are also able to estimate the decay-time constant from the resulting samples and obtain a mean value of 44 ns with an ~9 ns FWHM. In comparison, using digitized waveforms obtained at a 20 GSps sampling rate for the same LSO/PMT modules we obtain ~300 ps coincidence timing resolution, ~14% energy resolution at 511 keV, and ~5 ns FWHM for the estimated decay-time constant. Details of the results on the timing and energy resolutions by using the multi-threshold method indicate that it is a promising approach for implementing digital PET data acquisition.



## 1. Introduction

Recently, there is increasing interest in deriving relevant positron emission tomography (PET) event information from digitally sampled event waveforms [1–4], and we have investigated the potentials of employing such digital technologies in determining the event time. The developments in analog sampling techniques in the time domain, which samples the waveform at a regular time interval, have now made multi-GSps ($10^9$ samples per second) sampling possible [5,6]. As an alternative approach, we have also proposed a multi-threshold (MT) sampling method that samples the event waveform with respect to a small number of amplitude thresholds, and found the method to be capable of generating reasonably good timing resolution for time-of-flight (TOF) PET imaging [7,8]. In this paper, we present our prototype implementation of this MT sampling method in electronics. We also extend our analysis method to generate from the digitized waveform not only the event time, but also the event energy and the decay-time constant. Our results indicate that by employing four thresholds the MT sampling method can yield results that are useful for PET and TOF-PET imaging. In this digital data-acquisition (DAQ) architecture, all relevant information is derived from digital data generated in a unified sampling scheme. Conventionally in PET DAQ, event time and energy are processed separately using the constant fraction discriminators (CFD) and analog-to-digital converter (ADC). Those components can be eliminated in the MT sampling method. More advanced digital signal processing (DSP) techniques may also be explored to generate improved results. This simplified and unified approach, plus the possibility to explore advanced DSP technologies, may result in cost saving and improved event detection.

## 2. Methods

### 2.1. Prototype

Fig. 1 shows our prototype implementation of the MT sampling method. The prototype consists of two MT discriminator boards and a time-to-digital converter (TDC) board.

* Corresponding author. Tel.: +1 773 702 6276.
*E-mail address:* heejongkim@uchicago.edu (H. Kim).

0168-9002/$ - see front matter © 2009 Elsevier B.V. All rights reserved.
doi:10.1016/j.nima.2009.01.100

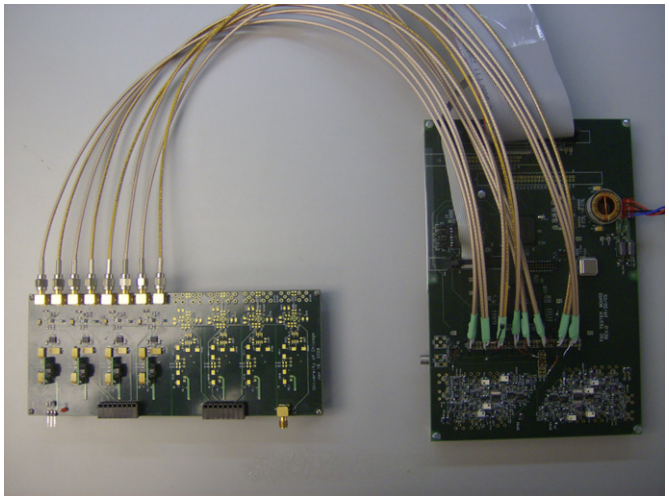

**Fig. 1.** A multi-threshold discriminator board (left) and the TDC board (right). The discriminator can provide up to eight thresholds for sampling its input signal. Currently, four channels have been implemented. The discriminator outputs are connected to the HPTDC chip on the TDC board. The HPTDC chip, developed at CERN, can provide eight TDC channels at 24.4 ps/bit resolution.

The MT discriminator board contains eight ADCMP582 comparators [9], each with a programmable voltage threshold that can be adjusted from 0 to 700 mV. These thresholds of the discriminator board were controlled by UMDDA-08HC from CyberResearch which is an 8-channel, 16-bit digital to analog converter. The input of the board is connected directly to a single photomultiplier tube (PMT) output with no pre-amplification applied. Currently, we have two MT boards and installed four comparators on each board. For digitization of the timing, the outputs of discriminators were connected to the High Performance TDC (HPTDC) ASIC which was developed at the European Organization for Nuclear Research (CERN) [10]. An HPTDC can provide eight channels with 24.4 ps/bit resolution. The HPTDC chip on the TDC board continuously took the outputs from the two MT discriminator boards and determined the digitized times when these output pulses made either low-to-high or high-to-low transitions. Either of the lowest threshold discriminator channel triggers data acquisition of TDC board. The timing data stored in 256 words deep FIFO of TDC were read out through a LabVIEW.

### 2.2. Experimental setup

Our setup for testing the prototype is depicted in Fig. 2. Two Hamamatsu R9800 PMTs coupled with LSO crystals ($6.25 \times 6.25 \times 25\,mm^3$) were spaced 5.0 cm apart, and an Na-22 positron source was placed in between the two PMTs. Both PMTs are operated at −1300 V to obtain a nominal gain of about $10^6$. Each PMT output was directly connected to one MT discriminator board input. The discriminator board currently provides four threshold levels and they were typically set at 50, 100, 200 and 300 mV.

In addition, the full waveforms of PMT signal and discriminator output were also taken by the Tektronix TDS6154C oscilloscope running at a 20 GSps sampling rate. These sampled waveforms were analyzed to investigate the timing characteristics of the MT boards, and to evaluate the performance characteristics of the prototype.

### 2.3. Analysis of the digital samples

Using the waveform samples generated by the MT board, we investigated the accuracy and precision in reconstructing the

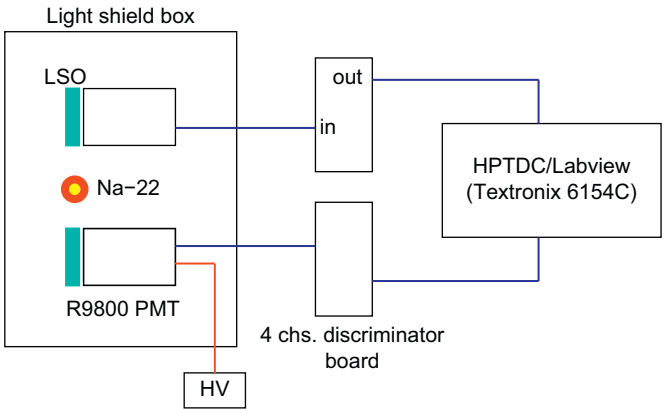


**Fig. 2.** Block diagram of the test setup. Four outputs from each discriminator boards were connected to HPTDC for time digitization. The PMT signals were directly fed to the oscilloscope to read out waveform.

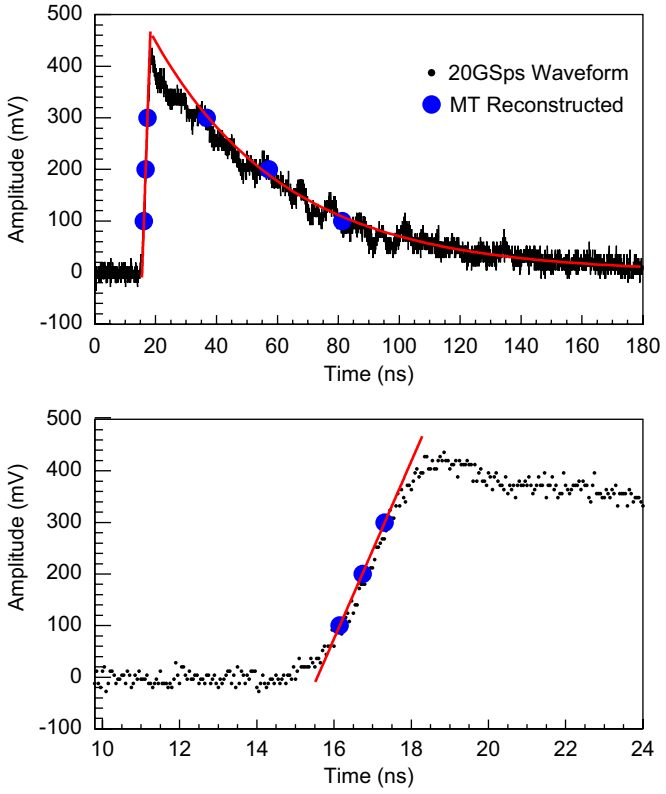


**Fig. 3.** Waveform vs. multi-threshold sampling. Samples acquired by the MT sampling are marked with big circle points. The line fitting on the rising edge and the exponential fitting on the trailing were applied to reconstruct the pulse shape. The waveform of PMT signal with 20 GSps sampling was shown with small circle points.

event pulse shape from the samples. The four thresholds currently used are 50, 100, 200 and 300 mV. To apply the MT method, events with at least two thresholds hits for each PMT were selected. Fig. 3 demonstrates the pulse shape reconstruction using the sampled points. The six timing points generated by the discriminator board are marked with big circle points. The line fitting was applied to the sampled points on the rising edge of the pulse, and the exponential curve fitting to the points on the decay portion of the pulse. The waveform of the same PMT signal was read out by the oscilloscope and superimposed in Fig. 3.

The event time and energy are determined from up to eight sampled points as follows: The points that comprise the rising edge are fit to a line, while the points on the trailing edge are fit to an exponential decay function. The intersection of the line fit to the rising edge with the zero-voltage level is defined as the event time of the pulse, the total area under the fitted line and exponential curve gives the event energy, and the exponential decay gives the scintillation decay constant. The event time, energy and scintillation decay constant are similarly determined by performing linear and exponential fittings to rising and decay portions of the event waveform digitized by the oscilloscope at 20 GSps. The correction on baseline level was done for the event timing and energy estimation for the 20 GSps waveform data analysis.

## 3. Results

### 3.1. Timing characteristics of the discriminator board

The signal path length from the input to the discriminators inside the board is different from channel to channel. Fig. 4 shows measured time differences between two discriminator outputs on the same discriminator board. In this measurement, a pulse generator output was used for the input to the board. The rise time and pulse height of input pulse were adjusted to about 2 ns and 400 mV, respectively, which were similar to R9800 PMT output in the setup. The thresholds were set at 100 mV for all the discriminator channels. The time differences have been measured for all installed channels on both boards; the average time resolution was estimated to 12.5 ps in FWHM for a single discriminator channel. The average time difference between the adjacent channels was measured ~200 ps that was consistent with an expectation from our HyperLynx simulations. The measured time differences between channels were used for the timing corrections in results reported below.

### 3.2. Energy resolution

Fig. 5 compares the pulse-height spectra obtained by using the MT method with four thresholds and by using the waveform digitized at 20 GSps. The integrated charges under the (reconstructed) pulse shape were calculated and shown in the figure. The events with 2, 3 or 4 threshold hit were used to make the energy estimation for the MT method. The results indicate a 18% energy resolution in FWHM at 511 keV with the former method, and 13% energy resolution in FWHM with the latter. Thus, the use of only four thresholds can already yield acceptable energy resolution for PET imaging.

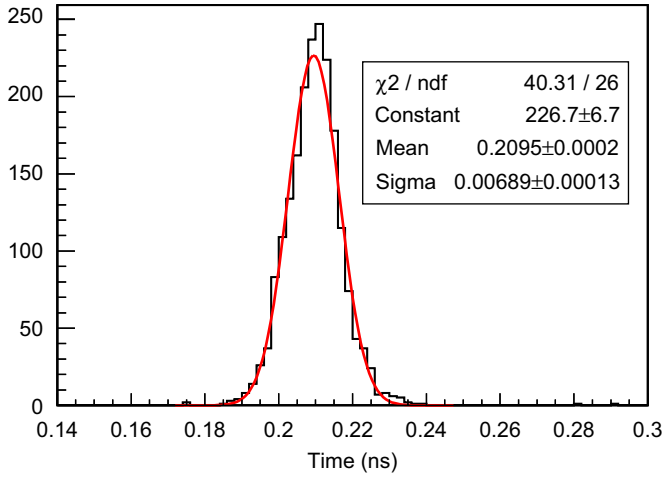


**Fig. 4.** A sample histogram showing the time offset between the outputs of two channels on the same multi-threshold board. The peak position gives the time offset between the two channels and the width shows the timing jitter, which is ~16.2 ps in FWHM in this case. The width of the other channel combination shows similar values, and the average timing jitter of a single channel was estimated to ~12.5 ps in FWHM.

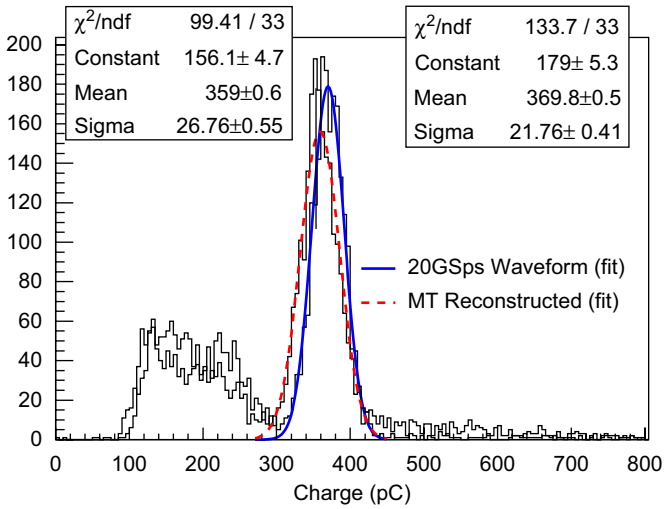


**Fig. 5.** Pulse-height spectrum obtained from the samples generated by our MT-sampling prototype (dashed curve), showing an ~18% energy resolution at 511 keV, and that from thousands of samples generated by using a Tektronix TDS6154C oscilloscope at 20 GSps (solid curve), showing an ~13% energy resolution at 511 keV. See Section 2.3 for the analysis methods generating the pulse height.

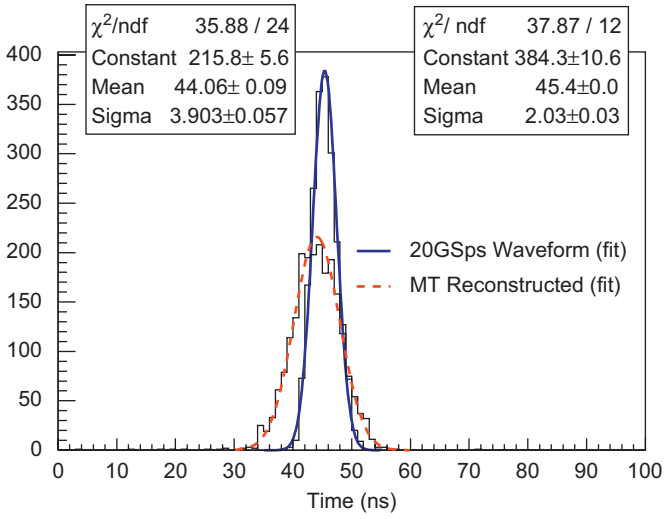


**Fig. 6.** The decay constant obtained from the samples acquired at the decay portion of the pulse generated by our MT-sampling prototype (dashed curve), showing a mean of ~45 ns and a width of ~9 ns FWHM, and that obtained from thousand samples acquired at the decay portion by using a Tektronix 6154C oscilloscope at 20 GSps (solid curve), showing a mean of ~44 ns and a width of ~4 ns FWHM. See Section 2.3 for the analysis methods generating the decay constant.

### 3.3. Decay-time constant

Fig. 6 shows the scintillation decay constants obtained. The events around the 511 keV peaks were kept for the figure by

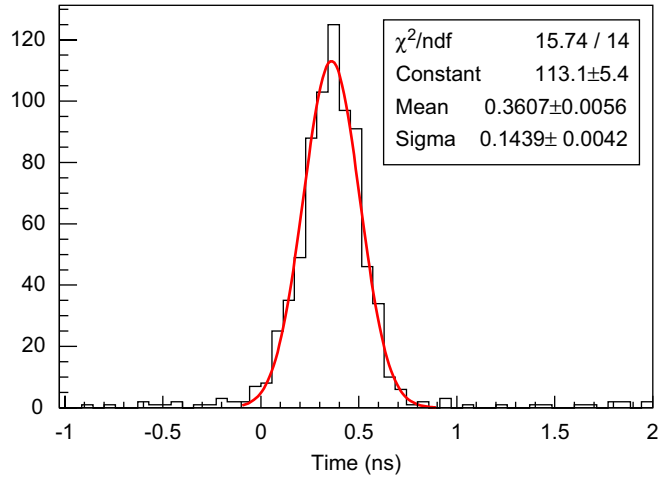


**Fig. 7.** The differential time in coincidence measurement obtained from two samples on the rising edge of the pulse generated by the MT-sampling prototype. The distribution shows a coincidence timing resolution of ~340 ps FWHM.

applying 90 and 114 keV energy window with respect to the peaks in Fig. 5 that correspond $3\sigma$ of the spectra. Using the digitized waveform, we obtain a mean value of 45 ns, with a width of ~5 ns FWHM. In comparison, by using four thresholds we obtain a mean value of 44 ns, with a width of ~9 ns FWHM. Thus, by using four thresholds we obtain an accuracy and precision that is promising for use in pulse shape discrimination.

### 3.4. Coincidence timing resolution

Fig. 7 shows the coincidence timing resolution using the MT method sampling method. The energy window of 114 keV with respect to 511 keV peak was applied. The zero crossing of the line fit on the rising edge points was regarded as the event time for each PMT signals. Fig. 7 shows a coincidence time resolution of about 340 ps in FWHM. On the other hand, the leading edge method using the lowest threshold (50 mV) alone gives ~390 ps timing resolution. We applied the line fit on the rising edges (50–300 mV region) to 20 GSps waveforms and obtained a coincident time resolution of about 300 ps in FWHM. To estimate the contribution on timing resolution from only the electronics and analyzing methods, the signal from the pulse generator was split into two and fed into the input of both discriminator boards. By following the same procedures to extract timing resolution, we estimated 74−88 ps of timing uncertainties coming from electronics and methods. The timing resolutions with three different methods are summarized in Table 1. These results can be compared to the previously reported ~300 ps of time resolution using the conventional analog CFD [8].

**Table 1**
Timing resolutions with different time extract methods.

| Method | Timing resolution (FWHM) (ps) |
|---|---|
| MT sampling | 340 ± 88 |
| 20 GSps waveform | 300 ± 80 |
| LE (20 mV) | 381 ± 76 |
| LE (50 mV) | 393 ± 74 |

The uncertainty includes only the contribution from electronics. The numbers in parentheses are threshold values used for the leading edge (LE) method.

## 4. Conclusion

An MT discriminator board was built to implement the scheme of sampling PET signals at the voltage domain. Timing outputs of the MT board with four thresholds were digitized by an HPTDC. The event timing and energy information was extracted from the reconstructed pulse shape using the sampled points. With the MT method, we obtained 18% of energy resolution and ~340 ps coincidence timing resolution. These results can be compared to 14% of energy resolution and ~300 ps timing resolution with 20 GSps waveform, for which several thousand data points are used to estimated the event energy and time. The MT sampling with four thresholds contributes ~40 ps degradation to coincidence timing and 4% degradation in energy resolution. It is possible that further improvements in timing can be achieved by threshold-level optimization and using more accurate fitting methods [11]. The current results shows that the MT sampling scheme that uses only eight data points per waveform has accuracy that is only slightly worse than that obtained by analog circuits or digital schemes that use thousands of data points per waveform. Thus, this is a promising method for implementing digital PET data acquisition.

## References

[1] M. Streun, G. Brandenburg, H. Larue, E. Zimmermann, K. Ziemons, H. Halling, IEEE Trans. Nucl. Sci. NS-48 (2001) 524.
[2] R. Fontaine, M.A. Tetrault, F. Belanger, N. Viscogliosi, R. Himmich, J.B. Michaud, S. Robert, J.D. Leroux, H. Semmaoui, P. Berad, J. Cadorette, C.M. Pepin, R. Lecomte, IEEE Trans. Nucl. Sci. NS-53 (2006) 784.
[3] P.D. Olcott, A. Fallu-Labruyere, F. Habte, C.S. Levin, W.K. Warburton, in: IEEE NSS/MIC Conference Record, 2006, pp. 1909–1911.
[4] A.R. MacFarland, S. Siegel, D.F. NewPort, R. Mintzer, B. Atkins, M. Lenox, in: IEEE NSS/MIC Conference Record, 2007, pp. 4262–4265.
[5] S. Ritt, Nucl. Instr. and Meth. A 518 (2004) 470.
[6] G. Varner, L. Ruckman, A. Wong, Nucl. Instr. and Meth. A 591 (2008) 534.
[7] Q. Xie, C.M. Kao, Z. Hsiau, C.T. Chen, IEEE Trans. Nucl. Sci. NS-52 (2005) 988.
[8] Q. Xie, C.M. Kao, X. Wang, N. Guo, C. Zhu, H. Frisch, W.W. Moses, C.T. Chen, in: IEEE NSS/MIC Conference Record, 2007, pp. 4271–4274.
[9] Analog Devices ⟨http://www.analog.com/⟩.
[10] J. Christiansen, High performance time to digital converter, CERN/EP-MIC, 2004.
[11] N. Petrick, A.O. Hero, N.H. Clinthorne, W.L. Rogers, IEEE Trans. Nucl. Sci. NS-41 (1994) 758.